KERNFORSCHUNGSZENTRUM

KARLSRUHE

November 1970 KFK 1316

Institut für Experimentelle Kernphysik

Developments in Cryogenic and Superconducting Magnets

F. Arendt, H. Brechna, J. Erb, N. Fessler, G. Hartwig, W. Heinz,
K.P. Jüngst, W. Maurer, G. Merle, G. Ries, W. Schauer,
J. von Schaewen, C. Schmidt, P. Turowski, A. Ulbricht

GESELLSCHAFT FUR KERNFORSCHUNG M. B. H.

KARLSRUHE

November 1970 KFK 1316

Institut für Experimentelle Kernphysik

DEVELOPMENTS IN CRYOGENIC AND SUPERCONDUCTING MAGNETS

Erratum

The name of a further author: G. Krafft

KERNFORSCHUNGSZENTRUM KARLSRUHE

November 1970 KFK 1316

Institut für Experimentelle Kernphysik

DEVELOPMENTS IN CRYOGENIC AND SUPERCONDUCTING MAGNETS+

by

F. Arendt, H. Brechna, J. Erb, N. Fessler, G. Hartwig, W. Heinz
K.P. Jüngst, W. Maurer, G. Merle, G. Ries, W. Schauer, J. von
Schaewen, C. Schmidt, P. Turowski, A. Ulbricht

Gesellschaft für Kernforschung m.b.H.

+Paper presented at the USSR Second National Accelerator Conference, 10 - 17 November, Moscow

Abstract

Present status of development work on superconducting and cryogenic magnets at the Institut für Experimentelle Kernphysik KFZ Karlsruhe is described. Based on experiments with multifilament conductors it was found that the theoretical prediction using Bean's model is confirmed down to 13 µm filament diameter. Test results of a d.c. superconducting quadrupole ($\frac{\partial B}{\partial r}$ = 37.2 T/m, with a warm aperture diameter of 0.12 m), design studies with superconducting ac dipole magnets with ferro magnetic return yokes are reported. Present work with pure aluminum tapes indicates, that Kohler's rule is not fulfilled at temperatures higher than 4.2 K. Discrepancy from theory is enhanced with purity. The relative magnetoresistance is higher with increased values of RRR.

Zusammenfassung

Der Status der Entwicklungsarbeiten auf dem Gebiet der supraleitenden und Tieftemperaturmagneten im Institut für Experimentelle Kernphysik, KFZ Karlsruhe, wird beschrieben. Experimentelle Untersuchungen an supraleitenden Multifilamentleitern, bestätigen die Theorie der Wechselstromverluste, die auf dem Bean-Modell basiert, bis zu Filamentdurchmessern von 13 µm. Über Testresultate eines supraleitenden DC-Quadrupols (Feldgradient 37,2 T/m mit warmer Bohrung von 0.12 m Durchmesser) wird berichtet. Konstruktionsentwürfe von gepulsten supraleitenden Dipolmagneten mit ferromagnetischer Eisenabschirmung werden beschrieben. Arbeiten mit hochreinen Aluminiumbändern zeigen, daß die Kohler-Gesetzmäßigkeit bei Temperaturen höher als 4,2 K nicht erfüllt ist. Die Abweichungen nehmen mit zunehmender Reinheit zu und der relative Magnetowiderstand wird größer.

I. INTRODUCTION

Superconducting pulsed current magnets are gaining in importance in future accelerators (proton synchrotrons) and in improving existing high energy systems. Directcurrent magnets allow the building of short beam lines for fast decaying particles, shielding and shaping magnetic fields, detection devices, magnets with large acceptance solid angle and magnets with high fields in large volumina. The operating cost of large experimental d.c. magnets is reduced substantially compared to water cooled conventional magnets with iron return yokes.

The generation of high magnetic fields (> 5 T) economically in superconducting pulsed dipole magnets allow the reduction of the synchrotron radius by about a factor of 3 to 4 compared to conventional machines which leads to considerable savings in capital cost for buildings, tunnels, experimental area etc.

High energy proton synchrotrons are more compact and possibly less expensive than conventional machines. This is especially true for very high energy machines with low repetition rates and a machine cycle with long flat top to obtain high duty cycles.

Prior to applying this new technology in an extended facility such as a proton synchrotron, considerable effort is necessary to solve pertinent problems inherent in superconducting devices: We summarize only a few: hysteresis losses in superconductors, cooling

phenomena, field distribution and field reproducibility, material performance and fatigue, irradiation problems, storage and distribution of high magnetic field energies (about an order of magnetude higher than in comparable conventional devices) handling large amounts of liquid helium in widely scattered vessels, complex safety and controle systems etc. This paper describes the work performed on superconducting and cryogenic magnets at the Institute of Experimental Nuclear Physics, Nuclear Research Center at Karlsruhe with the aim to utilize superconducting pulsed magnets in the conversion phase of the European (300 GeV) large accelerator (CERN II). Using a mixture of superconducting and conventional magnets the present proposal of the 300 GeV machine foresees a two stage buildingscheme. In the first stage a ringtunnel with a radius of 1100 m will be completed. For the separated function machine only the focussing magnets and a fraction of all required dipole coils will be installed to obtain an energy of 200 GeV. Between two bending magnets a space of 12 m is left free (Fig. 1) in which new magnets can be placed. During the first building stage (about 3 - 4 years after construction beginning) it will be seen if the pulsed superconducting research work has made sufficient progress that superconducting magnets could be placed in these open spaces. If this seems to be feasible the accelerator energy can be raised to 600 GeV. The second step is towards a conversion of all conventional magnets into superconducting ones. The magnet apertures are determined by the injection requirements and the structure of the 300 GeV machine: the existing CERN proton synchrotron is used as an injector. The machine structure has a FODO arrangement with 108 units, 6 insertions

and a Q value of 27.75 in both transverse directions. The required beam aperture has an extension of 10.2 cm in the horizontal and 4 cm in the vertical direction .

It will be necessary to test the magnets in a system (after having tested them individually), say of one half period of the CERN II synchrotron, or in a pilot accelerator with a particle energy in the GeV range. Following conditions have to be met by such a system of magnets:

1. The magnets must have an aperture size, a field rise time and flat top duration comparable to the final CERN II accelerator magnets.

2. To study systematically nonlinearity effects (fringing fields, field deviations in different magnets, aberrations etc.) the pilot system must be flexible enough to allow changes. The influence of various tolerances can be studied by adjusting beam parameters independent of other errors to obtain suitable corrections.

3. The final energy of a pilot accelerator must be in the GeV region. The system must be suitable for interesting high energy experiments such as accelerating deuterons.

The magnets being built for the pilot system will have a nominal length of about one to two meters. Combining several magnets in such a way to form long 6 ... 7 m units without loosing beam properties will be one of the more important tasks.

II. A REVIEW OF PROBLEMS AND ACHIEVEMENTS

At the present stage of superconducting magnet development, it is feasible to venture in building a larger magnet system to gain enough experience for the construction of a large accelerator such as CERN II. The wide range of diversified problems facing the magnet designer is given in short form below:

1. Slow Extraction and Required Field Tolerances in Magnets

Slow extraction of the beam, using the resonant method, is possible only if the field distribution in the main ring magnets is sufficiently linear. This means that for the proposed European 300 GeV accelerator the relative field error $S = \Delta B/B$ in the median plane (4 ... 5 cm extension) must be smaller than 1.5×10^{-3}. This is illustrated in Figures 2a) and 2b) showing the radial phase plane at the azimuth of the first septum in one of the lattices which have been considered. The plots are the output of a computer program [1] tracking four particles through each element of the ring and plotting their coordinates after each revolution. The initial coordinates are near the origin of the phase plane in the case of a third order resonance. A field error of less than 1.5×10^{-3} in the bending magnets due to a sextupole component (Fig. 2b) does not effect the extraction process seriously.

Augmenting the field error up to 2.5×10^{-3} (Fig. 2 b) yields complete stability. The particles remain within the admittance, which correspond to a septum position at 3 cm distance from the closed orbit, and, therefore, cannot be extracted in a satisfactory manner. Higher multipole components in the field expansion, giving the same field error, are less severe than the sextupole term [2]. A rms variation of the field value of 0.5×10^{-3} from one magnet to another can be tolerated in both, extraction and closed orbit distortions, only if closed orbit correction is applied. This is of course planned.

2. Joule's losses and conductor performance

One of the objectives of a cryogenic or superconducting accelerator, is low Joule's losses. These are encountered in superconductors, in the conductor substrate, in metallic structures (if any) and metallic dewars. The prototype synchrotron magnets are designed for high field performance (say nominal 4 ... 5 T). Losses measured in multifilament composite conductors are predictable with theory within measurements errors down to 10 µm filament diameter. Marked improvements are encountered in two different areas: The Joule's losses could be reduced by the introduction of multifilament, twisted composite conductors and the supercurrentdensity is improved considerably (about two fold) compared to values obtained commercially a few years back. Short sample critical current data versus external field perpendicular to conductor for a variety of commercially $Nb_{(x)}Ti$ conductors are given in Fig. 3. It is now feasible to achieve an overall coil current densi-

ty of about 2.5×10^8 A/m^2 at 5 T. In this number the coil packing factor is about 0.25 due to cooling channels and the cable design. When the coil is energized, the conductor is exposed to considerable Lorentz forces, which in unsupported and not reinforced condition surpass the yield strength of the superconductor ($\sim 10^4$ kp/cm^2) appreciably. Two ways of supporting the coil have been studied: reinforcement of the conductor by means of structural support and coil impregnation with suitable thermosets. The experiences with impregnated coils so far have not been satisfactory due to internal mismatch of the thermal contraction coefficient between the composite conductor and the thermoset. The conductor exhibits training and degradation.

Measurements of heat transfer in 0.4 m long vertical channels, 1.0, 1.5 and 2.0 mm gap height, and 40 mm width immersed in helium showed the transition from nucleate to film boiling at $\Delta T = 0.3 - 0.4$ K, while corresponding heat fluxes were in the range of 0.12 - 0.17 W/cm^2. The heat conductivity of superconducting coils impregnated in epoxy across the pancakes is 2×10^{-3} W/cm K at 4.5 K. With these data the height of individual impregnated pancakes was chosen to be 0.5 cm to obtain a temperature rise within the pancake of about 0.1 K or less. Thus the "hot spot" in impregnated coils will be about 0.4 ... 0.5 K higher than the bulk helium temperature. With these conditions, a field rise of 1.8 T/sec is feasible in magnets utilizing conductors with 10 µm filaments. At present the impregnated coil is preferred over reinforced not impregnated pancakes.

3. AC Losses in auxiliary parts of the magnet

When the magnetic field is changed at rates discussed (5 T/3 sec for 10 μm filaments), Joule's losses are encountered in all "non active" metallic parts, such as reinforcements, support structures, metallic bandages and specifically in the dewars. Some of the structural parts have to be of high strength metals , specifically nonmagnetic stainless steel, where eddy current losses can be generated. Although the resistivity in stainless steel is reduced only by a factor two, when the temperature is lowered from 300 K to 4.2 K, the total induced losses are high enough, to be of concern. The measures taken are to eliminate if possible all high strength metallic parts by employing unidirectional glass-thermoset (semi cured) tapes, and by means of high strength non-metallic structural materials.
The preliminary design of the coil dewar foresees a box type structure, where the forces between coil and flux return path (iron yoke) is taken by flanges located at the ends of individual dewar sections. The glass epoxy dewar must be equipped with non permeable liners, which prevents the penetration of heliumgas through the structure, or the outgassing of epoxies into the vacuum space.

4. Irradiation study

The superconducting magnet is exposed to nuclear radiation by a number of reasons:

a) Missteering of beams

b) Production of secondary energetic particles close to slits or collimators

The effect of irradiation and long range performance of magnets is of considerable interest and is investigated presently by irradiating small coils with 50 MeV deuterons at (4 ... 5) K.

The effect of electron, neutron, proton and deuteron irradiation on the J_c-B_c characteristic of superconductors type II, such as $Nb_{(x)}Ti$ and Nb_3Sn is reported by several investigators [3...7]. When irradiated, T_c and H_c are reduced. J_c is changed but a definite prediction of changes in J_c is difficult. In some materials such as Nb_3Sn diffusion film the critical current density is enhanced about sixfold, when irradiated with 3 MeV protons. In $Nb_{(x)}Ti$ the critical current density is even reduced.

The enhancement of J_c as a function of irradiated dose rate does not occur uniformly over the entire coil, but is a localized phenomenon. The conductor J_c-B_c characteristic is changed in a localized area yielding more embrittlement and specifically to a more "flux jump" sensitive condition. Temporary external or internal disturbances may lead to a "normality" zone, as the substrate is also affected by irradiation (copper is work hardened and the electrical resistivity increased) [8]. The weakest link in the coil is the interturn insulation, especially if organic materials are used to impregnate the coils. A "normality" zone may lead to a short circuit between turns (due to carburized insulation), a shift in the energy distribution over the coil and finally to a

magnet quench. Some improvements in the behaviour of organic insulations (mechanical and electrical) are encountered at low temperature [9], but these are not enough to warrent safe operation of magnets with present designs, if no preventive measures are taken and new designs conceived.

5. Flux return path

The positioning of the iron yoke around the coil, its shape and its influence on field distribution is of considerable importance in the magnet performance. The iron yoke can be placed in close proximity to the coil and must be cooled down to liquid helium temperature. Theoretical investigations indicate that in this case the field contribution due to iron is maximum, field shielding is effectiv, but if the iron is not properly shaped, field distortion in the useful aperture is encountered [10]. The advantages of the solution are, that there are no forces transmitted to the dewar due to relative positioning of coil and iron, and that the dewar can be built mainly from nonmagnetic stainless steel, where only the portion of the magnet aperture must be built either from a corrogated tube with low ac losses or a nonmetallic filamental structure. The disadvantage of this scheme is the excessive helium requirement for cool down (enthalpy cooling is practically impossible) and the hysteresis and eddy current losses in iron which are added to the superconducting ac losses in the coil and must be removed by the coolant.

If the iron yoke is placed around the dewar, the iron field contribution is small, the forces due to eccentric location of coil and iron yoke transmitted to the dewar could be excessive, but the iron influence on the field distortion is reduced. The iron ac losses are of no consequence at room temperature. Both solutions are presently studied at Karlsruhe. The iron in proximity of the coil is used with a high purity aluminum dipole, while the iron around the dewar is foreseen for the superconducting dipole magnet.

6. Cryogenic Magnets

High purity aluminum tapes have low losses and may be attractive for low frequency cryogenic magnet applications [11] as well as substrates for multifilament superconductors, current leads and other cryogenic applications. Specifically loss rates at liquid hydrogen are of interest: Aluminum tapes with a residual resistivity ratio of RRR = 10^4 in tapes (RRR $\equiv \rho(300K)/\rho(4.2K)$ are commercially available and are being utilized at Karlsruhe in a dipole coil 0.4 m long. Although magnetoresistance measurements at liquid hydrogen temperature show that ac-losses in the coil are about an order of magnitude higher than in comparable superconducting coils at 4.2 K, the application of aluminum tapes may very well be attractive at frequencies, where losses in the superconductors become exorbitant.

III. SUPERCONDUCTING MAGNETS

Currently two types of magnets are being investigated:

a) Superconducting ac dipole magnets

b) Superconducting dc quadrupole magnets

Some of the more important test results in both directions are given below:

1. Superconducting ac dipole magnets

With the aim to build a pulsed superconducting accelerator magnet, a series of preliminary tests were performed in various sized coils ranging up to 2 kJ stored field energy. Theoretical investigation of ac losses in superconductors are persued parallel to experiments performed on multifilament composite conductors.

To derive theoretical ac loss values in a magnet, Beans's critical state model was chosen. Using a computer program, the coil ac losses are obtained by subdividing the coil volume into a large number of small elements, each being exposed to a constant field. Considering in addition the eddy current losses in the substrate, the theoretical values agree with experimental data down to filament diameter of 13 µm within 20 % [12].

The J-B relations (see Fig. 3) are assumed to be either linear, hyperbolic or exponential according to the type of $Nb_{(x)}Ti$ selected. Estimated

losses in a one m long 5 T dipole magnet (8 x 11 cm aperture) are given in Fig. 4. Losses per cycle are plotted versus $J_0 B_0 d$, where J_0 and B_0 are the characteristic parameters of J(B) relation and d is the individual filament diameter [13].

The dotted lines yield the relation between $J_0 B_0 d$ and the current density in the superconductor for various filament diameters, assuming that at 5 T the critical short sample current value in the filaments has just been reached.

The reduction of ac losses by increasing the current density is small. However, increasing the overall current density in the coil to the possible attainable limit is of course to reduce the amount of conductor material required in a magnet, to decrease outer coil dimensions and reduce the stored field energy. A preliminary design of a superconducting dipole magnet is given in Fig. 5. The magnet useful aperture is cold. The winding aperture is 8 x 11 cm, the iron yoke inner diameter 40 cm is placed around the dewar, which is in this case presumed to be made on glass epoxy basis. The coil cross-section is an approximation of two intersecting ellipses. The actual coil arrangement and the dimensions of individual pancakes are obtained from a computer program optimizing each element for small field errors for the given number of pancakes. The calculations indicate that for the magnet shown the field deviation within the dotted circle (d = 6 cm) is $\Delta B/B = 2 \times 10^{-4}$. The relative field error encountered by the displacement of a pancake by 0.1 mm in horizontal direction is about 6×10^{-4} which already places stringent requirements on coil tolerances, the accuracy of

coil winding as well as coil support. The magnetomechanical forces on the conductor of the 1 m long dipole are approximately 2×10^5 kp and thus to prevent wire movements, impregnation with suitable thermosets seems inevitable.

The selection of appropriate resins, to match conductor thermal contraction is presently a major problem. Coil support structure is composed mainly of nonmetallic high strength glass fiber epoxy tapes and bandages.

While in Fig. 5 the pancake arrangement with horizontal coolant passages was shown which may pose some cooling problems, Fig. 6 shows an alternative solution with vertical channels, which yields good heat transfer values. The computed field homogeneity within the 6 cm diameter circle is comparable to the values obtained in Fig. 5. Much thought has been devoted to coil ends which do effect the field homogeneity. If the coil ends are bend 90° to the coil longitudinal axis and the straight (parallel to the longitudinal axis) sections are of equal length, the $\int Bdl$ over the useful coil aperture will be constant.

To study winding and potting techniques a series of test dipole pancakes has been manufactured. A full size copper model (1 m overall length) was built similar to the arrangement of Fig. 5 to study the effect of coil tolerances on field distributions. Using square insulated hard copper conductors variations in the thickness of individual pancakes were within $\pm$ 70 µm.

Due to different mechanical properties of composite superconductors compared to copper and to obtain the stringent tolerances required in (II. 1) a series of pancakes with composite multifilament conductors impregnated in suitable thermosets are currently being manufactured.

2. Superconducting dc quadrupole

To study the performance of a large superconducting beam transport magnet and to obtain data on optical properties (first and second order), short and long range coil behaviour, a one (1) meter quadrupole with a warm bore (12 cm diameter) was designed and built [14]. The coils are wound from 1.5 cm wide and 0.15 mm thick Nb_3Sn tape cladded with 0.05 mm thick copper strips on both sides. The conductor is edge cooled.

The magnet is placed horizontally in a dewar having static heat losses (magnet and dewar) of 5.8 l/hour, while the total losses, when the magnet is energized are 6.2 l/hour helium.

To cool down the quadrupole, liquid nitrogen was applied to cool the magnet and its auxiliary parts to $\sim$ 80 K. Roughly 110 liters of LN_2 were used during the cool down time of 2 hours. Successive evaporation of LN_2 and final evacuation were performed in 1.5 hours. The magnet-temperature was then about 100 K. Cooling down to 4.2 K and filling the helium container was performed in 2.5 hours while 220 liters of helium were used. The weight of all parts to be cooled was 220 kp. The helium container can store 60 liters of helium.

When the magnet was energized the quench current of 990 A was reached which corresponds to a field gradient of 37.2 T/m, while the design number was 1300 A producing 50 T/m. At the design current the field at the conductor would have been 3.9 T (coil inner diameter is 15.5 cm).

In Fig. 7 the short sample data for Nb_3Sn are given in the shaded area, while the measured quench currents lay way below expected short sample values.

The coil is well supported and it is not beleaved that conductor movements may trigger an earlier unexpected quench indicating conductor degradation. No training was observed up to date. Reasons for the measured low gradient cannot be given with certainty. The unstable conductor performance may be due to poor heat transfer characteristics of the coil, but two and three dimensional field computation indicate a field component of 2.7 T at 990 A perpendicular to the width of Nb_3Sn tape in the region between adjacent poles and at the coil ends. At fields higher than 2 T perpendicular to the tape width Nb_3Sn becomes unstable [15,16]. The field gradient measured in the radial direction is constant within 10^{-2} over the warm magnet aperture.

Measuring the field along the longitudinal quadrupole axis showed a periodic field variation of $\Delta B/B = 2 \times 10^{-3}$ (Fig. 8a,b). The length between maximum $\Delta B/B$ variation corresponds to the location of stainless steel reinforcements being placed at 6.5 cm distance from each other. The field error may be due to local coil distortion, but may also be attributed to some ferromagnetic austenetic behaviour of stressed stainless steel at 4.2 K [17].

IV. CRYOGENIC MAGNETS

Aluminum is one of those materials which has so far shown best cryogenic performance with respect to magnet application. Using processes such as organo-electrolysis and zone refining a residual resistivity ratio of several ten thousand could be achieved in bulk material. Copper can be produced with the same purity as Al but its magnetoresistance increases rather linear with field and is thus not suitable, while saturation effects are observed at higher magnetic fields for aluminum.

Studying the applicability of Al conductors in pulsed cryogenic magnet design measurements of the resistivity behaviour were performed in small tape-wound (12 x 0.3 mm^2) pancakes with inner and outer diameter of 4 cm and 12 cm, respectively. The tapes were insulated with a 25 µm thick Hostaphan[+] foil.

In this configuration a variety of tapes in the residual resistivity range of $1600 \leq RRR_{bulk} \leq 11{,}700$ were measured at 4.2 K and 20.4 K. For high purity tapes with a thickness of d = 0.3 mm the size effect is obvious. The size effect correction for completely diffuse surface scattering (p = 0) is calculated according to the theory of Sondheimer [18]:

$$\rho_{tape} = \rho_{bulk} \frac{\phi(d/\ell, p)}{d/\ell} \qquad (1)$$

[+] trade name (Hostaphan, polyäthylenterephthalat-foil), Kalle-AG.

For the electron mean free path ℓ the average value of several measurements, $\rho_{bulk} \cdot \ell = 7 \times 10^{-12}$ Ohm·cm^2, was used in our calculation. The integral $\phi(d/\ell,p)$ was obtained from numerical calculations of Dworschak et al. [19]. With these numbers a residual resistivity ratio of $RRR_{bulk} = 11{,}700$ is reduced to $RRR_{tape} = 8000$ for a 0.3 mm tape.

According to Matthiessen's law the resistivity is obtained by adding a temperature independent residual part and an intrinsic part, which is proportional to T^5:

$$\rho(T) = \rho_r + \bar{\rho}_i \cdot T^5 \qquad (2)$$

The residual resistivity is obtained from electron-scattering on defects and the intrinsic resistance from electron-phonon interaction. The latter part is practically negligable at 4.2 K. Fig. 9 shows that both effects are not independent and the Matthiessen law is violated. The resistivity difference $\rho(20.4\ K) - \rho(4.2\ K)$ from several experimental results [11,20,21] have been plotted versus the residual resistivity ratio. The interaction between dispersion phenomena is increased with defect concentration.

According to Kohler the relative change in resistivity

$$\Delta\rho/\rho = (\rho(B,T) - \rho(0,T))/\rho(0,T)$$

is a function of B/ρ only. According to a two-band model the change in resistivity may be written in the form:

$$\frac{\Delta\rho}{\rho} = \frac{\alpha(B/\rho)^2}{1 + \beta(B/\rho)^2}\ , \qquad (3)$$

where α and β are material constants. Deviations from Kohler's rule, which is based on isotropy of scattering processes, were found in function of temperature and impurity content for polycrystal Al [11,20] and for single crystals [21,22]. In Fig. 10 the relative resistivity increase is plotted versus magnetic field. In our measurements the self field values given, are half of the central coil field as a rough approximation for comparison with short sample measurements. The qualitative agreement is quite satisfactory showing that with increasing purity the magnetoresistance is increased markedly. Saturation effects are observed at fields higher than 3 T. Measurements of Fickett [20] indicate even a linear part in the magnetoresistance curve at 4 T.

The temperature variation of the magnetoresistance and the effective resistivity ratio RR_{tape} (B,T) for the different purities investigated at 4.2 K and 20.4 K are shown in Fig. 11.

Single crystal measurements for specific angular directions between crystallographic axis and external field show saturation effects in several orientations, in others the anomaleous non-saturating behaviour of the magnetoresistance is not yet understood. Probably several phenomena are acting together such as small angle electron-phonon scattering [23], magnetic breakdown in specific crystal directions [24] or the generation of neck-like channels to neighbouring Brillouin zones [25], which remove electrons from the conductivity mechanism.

The anomaleous resistivity behaviour is in so far disturbing, as aluminum may be used at liquid hydrogen temperature in magnets. Thus more systematic experimentation is indicated, mainly in studying the temperature and purity dependence of the magnetoresistance. For this purpose short sample measurements are being prepared for tests under conditions expected in a high field magnet.

Parallel to the short sample investigations a window frame type magnet is currently being constructed (Fig. 12), which is designed to produce a field of 4 T in 4 x 5 cm^2 aperture of 40 cm length. Al-tape of 8 x 0.3 mm^2 crossection, insulated with an aluminumoxyd surface of 5 µm thickness, will be used with a tape-RRR of 10000. Tests for bending the race-track coils to a saddle form have been performed successfully. The testmagnet will be operated at different cryogenic temperatures and pulse frequencies, for which the overall losses will be measured.

Extrapolation of magnetoresistance to 4 T from our previous measurements indicate that we may expect approximately 180 W dc-losses at 4.2 K and 1000 W dc-losses at 20.4 K. These values corresponds to a gain in overall power of 7 at 4.2 K and 13 at 20.4 K, assuming a refrigerator efficiency relative to ideal thermodynamic efficiency of 0.15 at 4.2 K and 0.3 at 20.4 K.

FIGURES

1. Schematic view of the missing magnet-semiperiod (CERN II) with and without superconducting magnets.

2. Phase plane diagram at the first septum
S = Sextupole field error.

3. Short sample J_c-B_c characteristics of various $Nb_{(x)}Ti$ conductors.

4. Hysteresis losses in a one meter superconducting ac dipole.

5. Design of an ac dipole magnet (5.54 T, 50 kA/cm^2 overall current density, 8 cm x 11 cm winding aperture, cold bore)

6. Computer-generated dipole configuration giving 5.36 T with an overall current density of 50 kA/cm^2.

7. Current, field characteristics of the 12 cm diameter Karlsruhe quadrupole.

8.a Field homogeneity parallel to the z-axis at r = 4.95 cm in the space between adjacant poles (I = 950 A).

8.b Field homogeneity parallel to the z-axis as in Fig. 8a but with 32 times magnification

9. Deviation from Matthiessen's rule in aluminum. Experimental values of $\rho_{bulk}(20.4\ K) - \rho_{bulk}(4.2\ K)$ plotted versus bulk residual resistivity ratio.

10. Magnetoresistance of Al at 20.4 K.

11. Resistivity measurements in pancakes.

a) the relative increase of resistivity at the central coil field plotted versus B_{centr} for 4.2 K and 20.4 K and a tape with a bulk residual resistivity ratio of 11,700

b) the effective pancake resistivity ratio at a central coil field of 2.5 T plotted versus purity (bulk residual resistivity ratio) for 4.2 K and 20.4 K.

12 Central field of the Al-testmagnet.
The testmagnet, 40 cm in length, will be mounted with vertically positioned coolant channels. The iron yoke (outer diameter ∿60 cm) is cooled together with the tape wound saddle coils.

REFERENCES

1. J. Erb and G. Merle
KFK 3/69/26 (1969), Karlsruhe

2. J. Erb and G. Merle
to be published

3. H.J. Bode, K. Wohlleben
Zeitschr. f. angewandte Phys. 27, 92 (1969)

4. G.W. Cullen, R.L. Novak
J. appl. Phys. 37, 3348 (1966)

5. H.T. Coffey, E.L. Keller, A. Patterson, S.L. Autler
Phys. Rev. 155, 355 (1967)

6. H. Ullmaier
Zeitschrift f. angewandte Phys. 26, 261 (1969)

7. C.P. Bean, R.L. Fleischer, P.S. Schwartz, H.R. Hart
J. Appl. Phys. 37, 2218 (1966)

8. H. Brechna
Proc. 1968 Brookhaven Summer Study, part III,1011 (1968)

9. E.E. Kerlin, E.T. Smith
FZK 290 (1966)

10. J. von Schaewen, H. Brechna
to be published

11. W. Schauer, W. Specking, P. Turowski
Proc. 3rd Magnetic Technology Conference Hamburg (1970)

12. K.P. Jüngst, G. Krafft, G. Ries
Proc. 3rd Magnet Technology Conference Hamburg (1970)

13. G. Ries
BSG Notiz 7019 (1970) KFZ-Karlsruhe

14. N. Fessler, G. Bogner, H. Kuckuck, D. Kullmann
Proc. 3rd Magnet Technology Conference Hamburg (1970)

15 M.N. Wilson
Rutherford Lab. RPA/A 73, 5 (1969)

16. H. Brechna
SLAC TN, 10, 1 (1970)

17. D.C. Larbelestier, H.W. King
Cryogenics, Vol. 10, No. 4,410 (1970)

18. E.H. Sondheimer
Adv. Phys. 1, 1 (1952)

19. F. Dworschak, W. Sassin, J. Wick, J. Wurm
KFA Jülich, Jül - 575-FN (1969)

20. R.F. Fickett
NBS Boulder, Col. to be published

21. E.S. Borovik, V.G. Volotskaya, N.Yu, Fogel
Sov. Phys. JETP, 18, 34 (1964)

22. Y.N. Chiang, V.V. Emerenko, O.G. Shevchenko
Sov. Phys. JETP, 30, 1040 (1970)

23. A.B. Pippard
Proc. Royal Soc. 305A, 291 (1968)

24. R.J. Balcombe, R.A. Parker
Phil. Mag. 21, 533 (1970)

25. R.A. Young Phys. Rev. 175, 813 (1968)

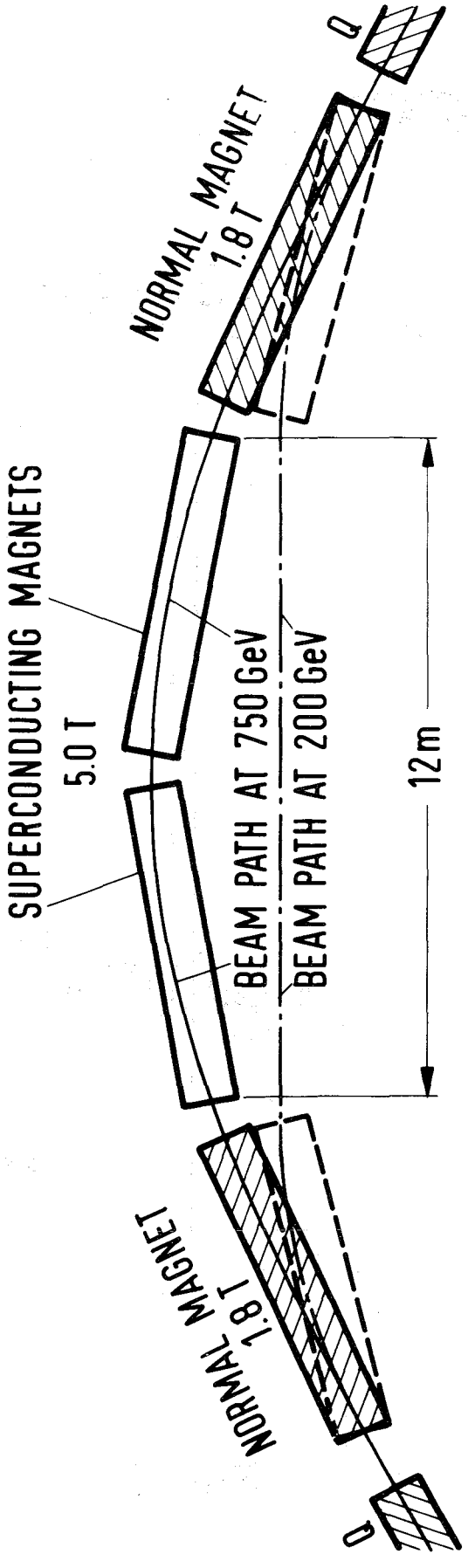
Q
NORMAL MAGNET
1.8 T
SUPERCONDUCTING MAGNETS
5.0 T
BEAM PATH AT 750 GeV
BEAM PATH AT 200 GeV
12 m
NORMAL MAGNET
1.8 T
Q

Fig. 1

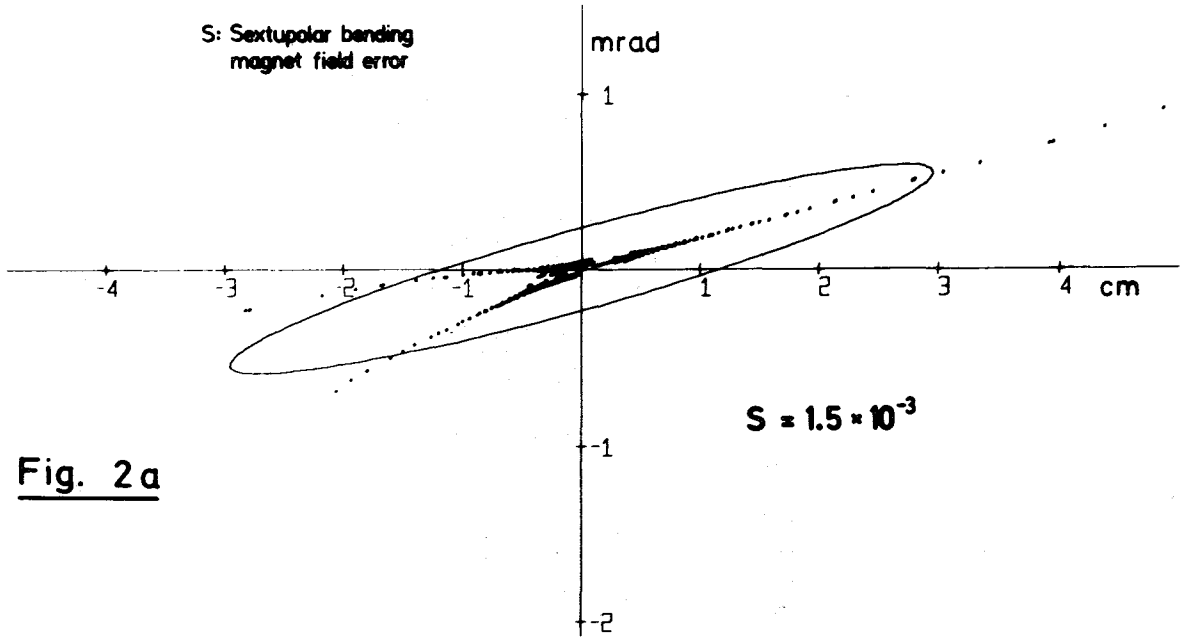

Fig. 2a

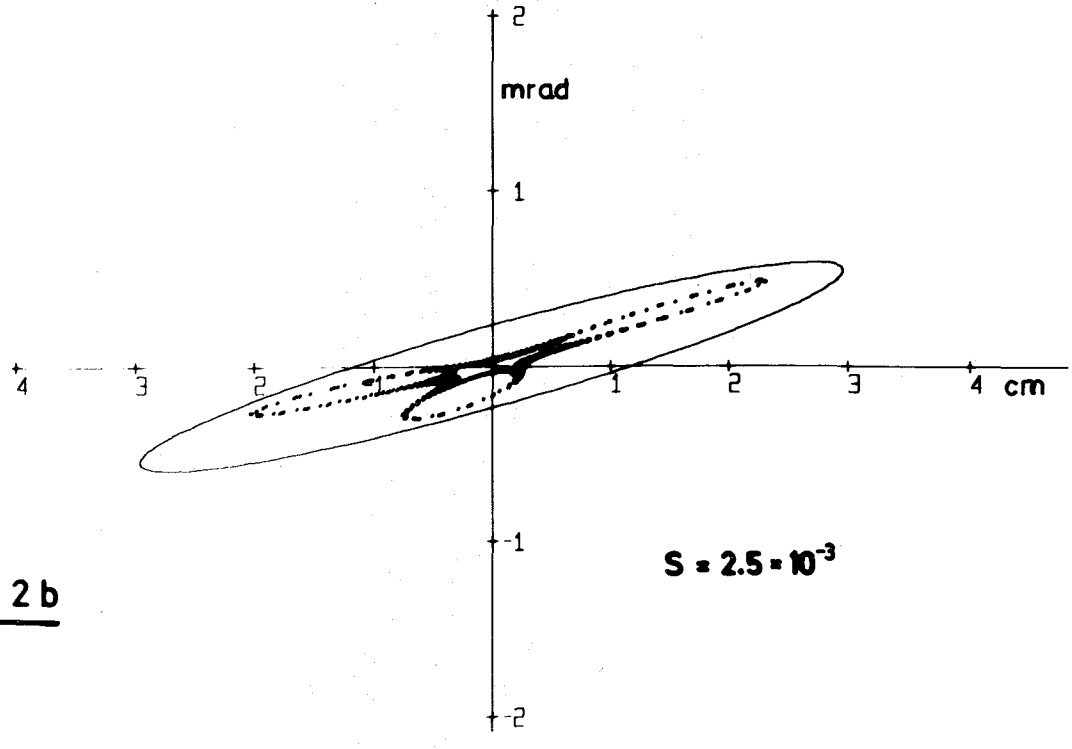

Fig. 2b

Fig. 2

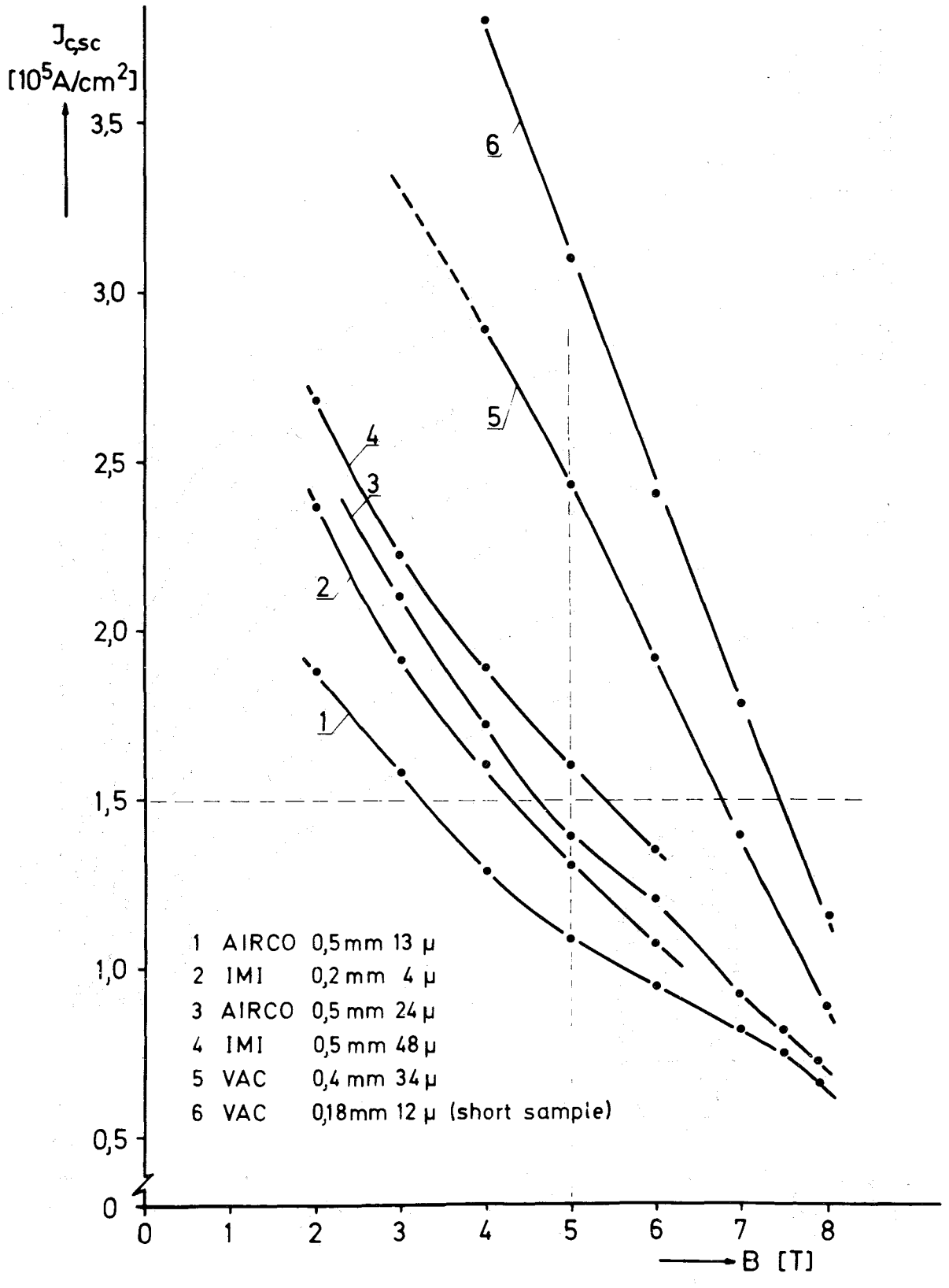
$J_{c,sc}$
[10^5A/cm^2]
3,5
3,0
2,5
2,0
1,5
1,0
0,5
0
0
1
2
3
4
5
6
7
8
B [T]
1
2
3
4
5
6
1 AIRCO 0,5mm 13 µ
2 IMI 0,2 mm 4 µ
3 AIRCO 0,5 mm 24 µ
4 IMI 0,5 mm 48 µ
5 VAC 0,4 mm 34 µ
6 VAC 0,18mm 12 µ (short sample)

Fig. 3

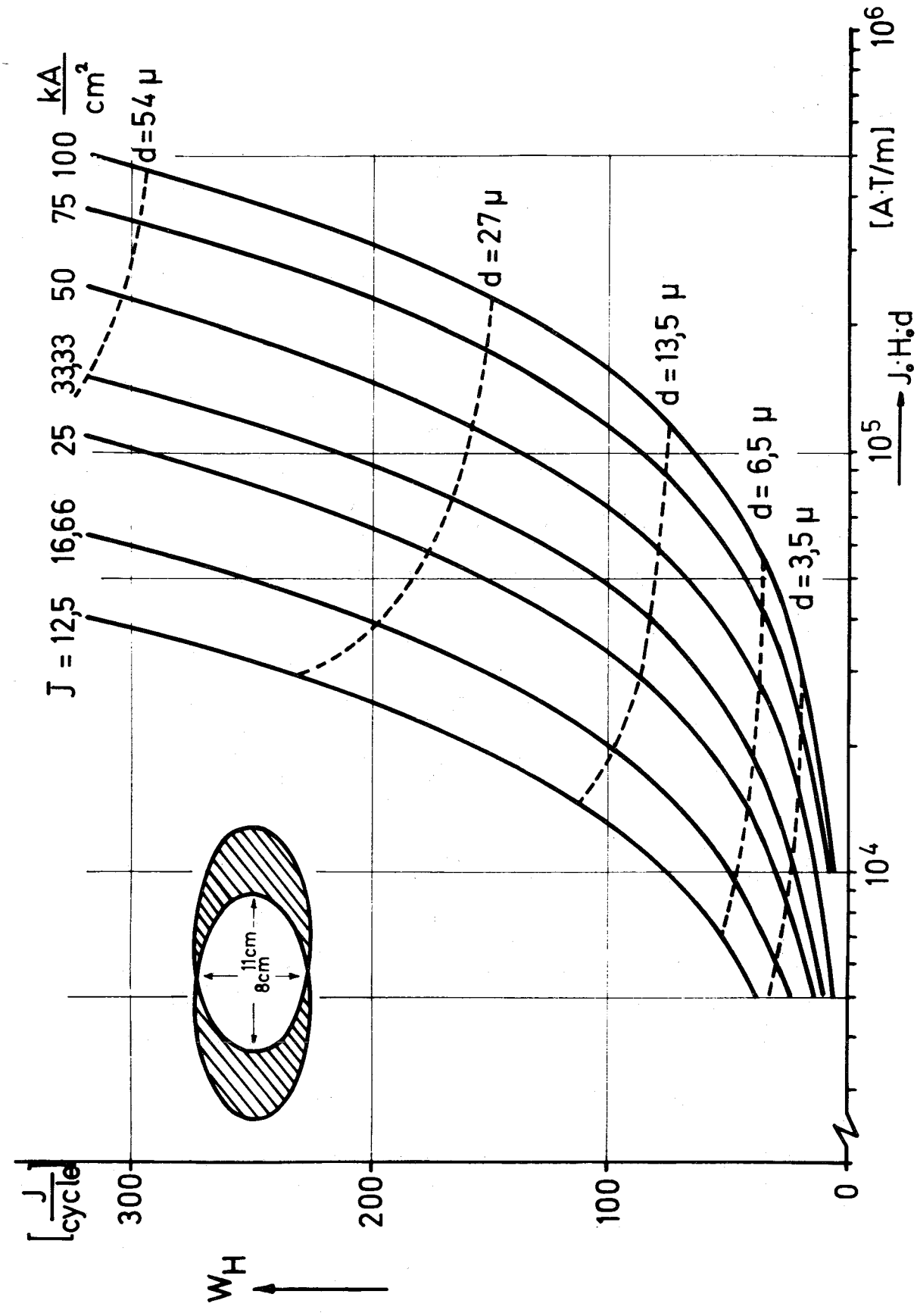
J = 12,5
16,66
25
33,33
50
75
100
kA/cm²
d=54 µ
d=27 µ
d=13,5 µ
d=6,5 µ
d=3,5 µ
11cm
8cm
W_H
J/cycle
300
200
100
0
10⁴
10⁵
10⁶
J₀·H·d
[A·T/m]

Fig. 4

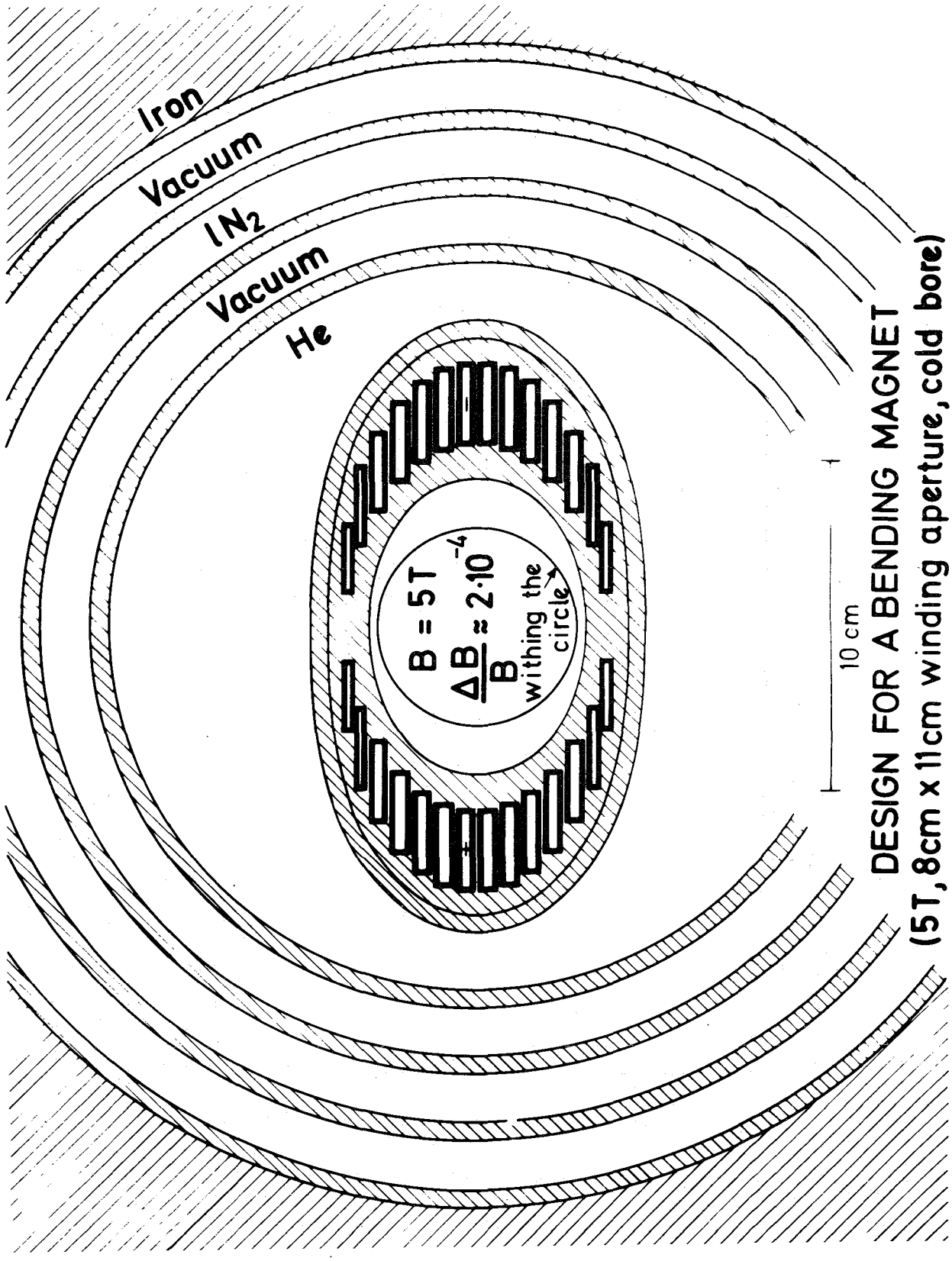
Iron
Vacuum
lN_2
Vacuum
He
B = 5T
$\frac{\Delta B}{B} \approx 2 \cdot 10^{-4}$
withing the circle
10 cm
DESIGN FOR A BENDING MAGNET
(5T, 8cm x 11cm winding aperture, cold bore)

Fig. 5

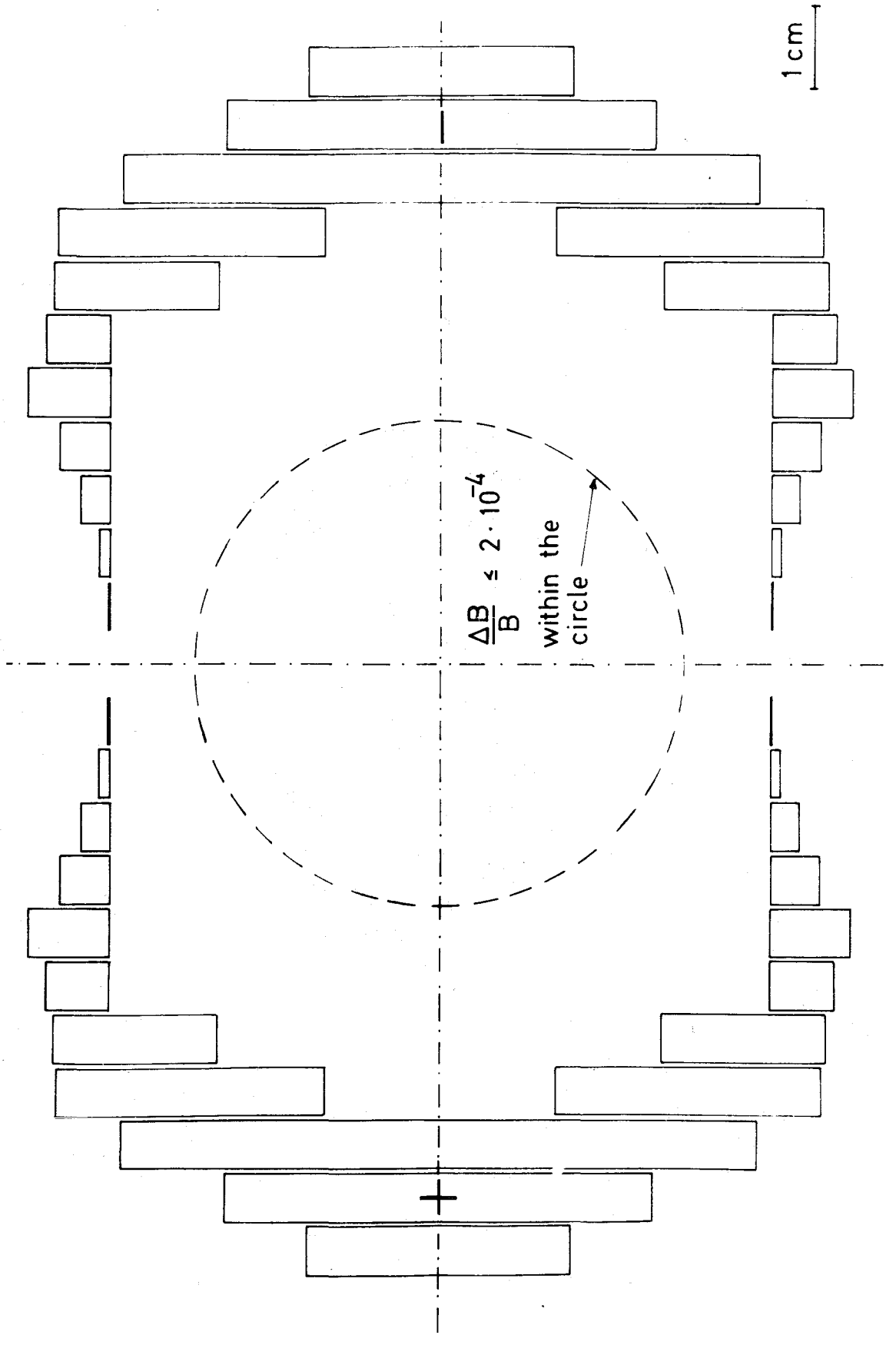

Fig. 6

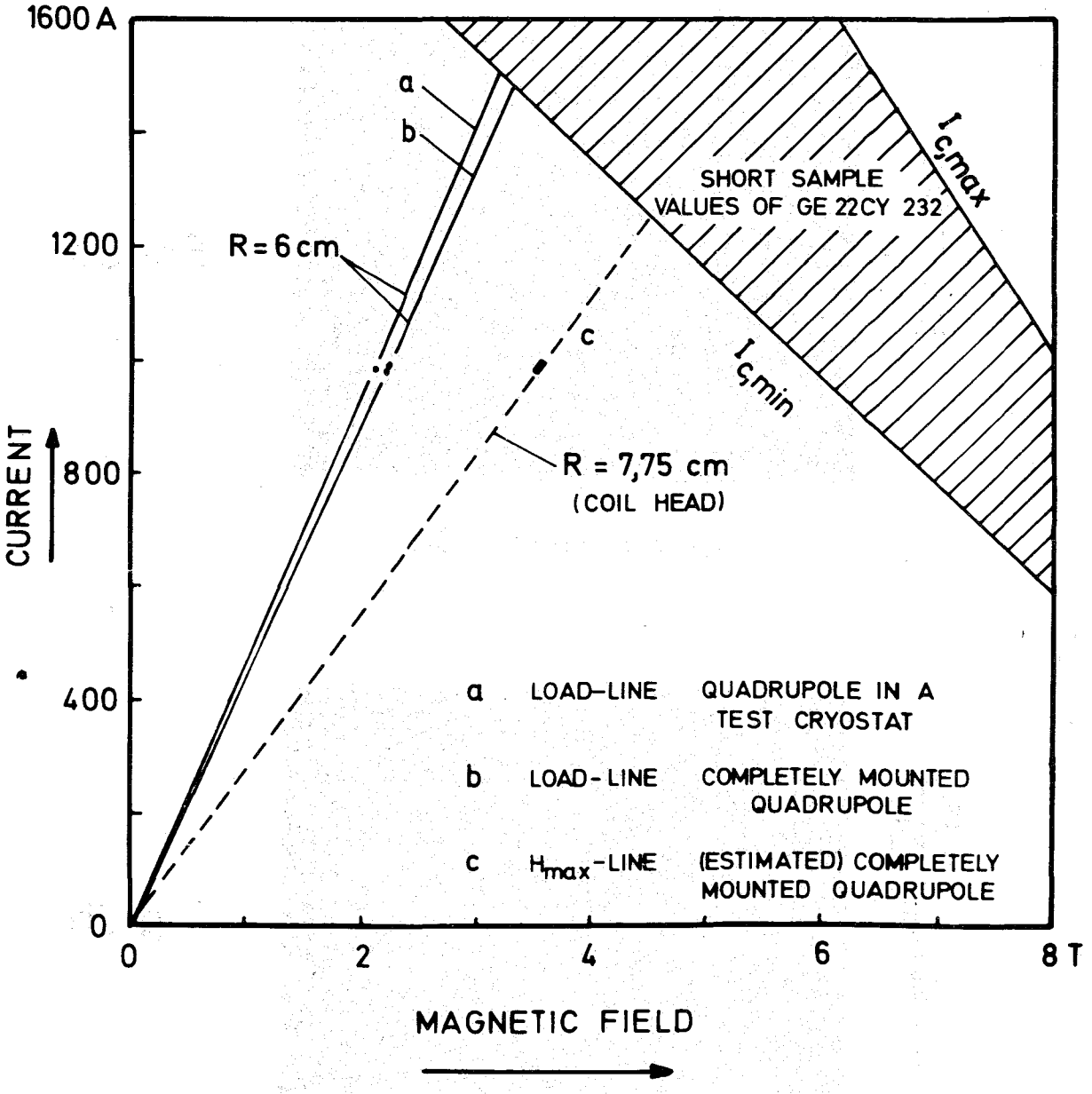
1600 A
1200
800
400
0
CURRENT
a
b
c
R = 6 cm
R = 7,75 cm
(COIL HEAD)
SHORT SAMPLE
VALUES OF GE 22CY 232
Ic,max
Ic,min
a LOAD-LINE QUADRUPOLE IN A TEST CRYOSTAT
b LOAD-LINE COMPLETELY MOUNTED QUADRUPOLE
c Hmax-LINE (ESTIMATED) COMPLETELY MOUNTED QUADRUPOLE
0
2
4
6
8 T
MAGNETIC FIELD

Fig. 7

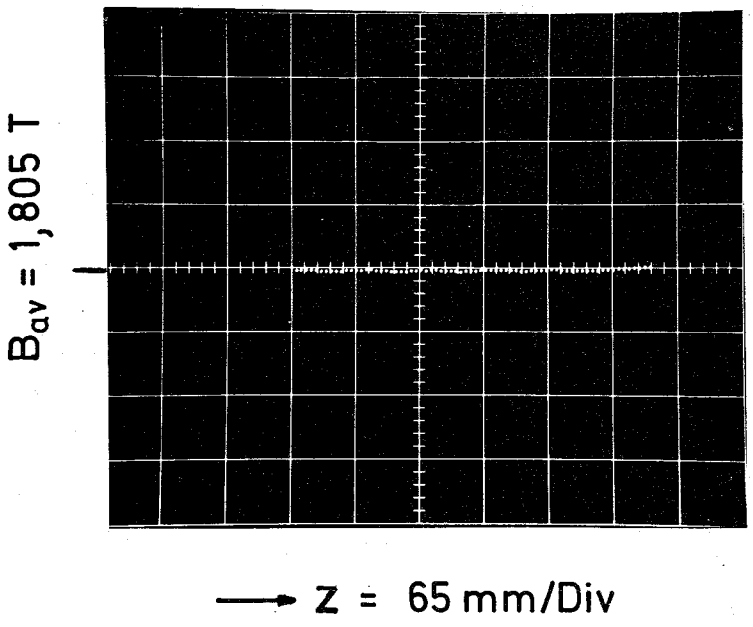

Fig. 8a

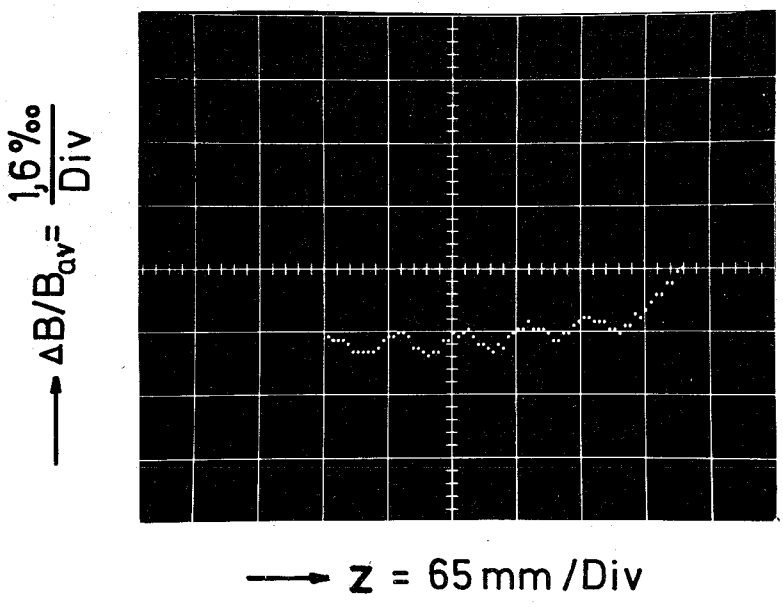

Fig. 8b

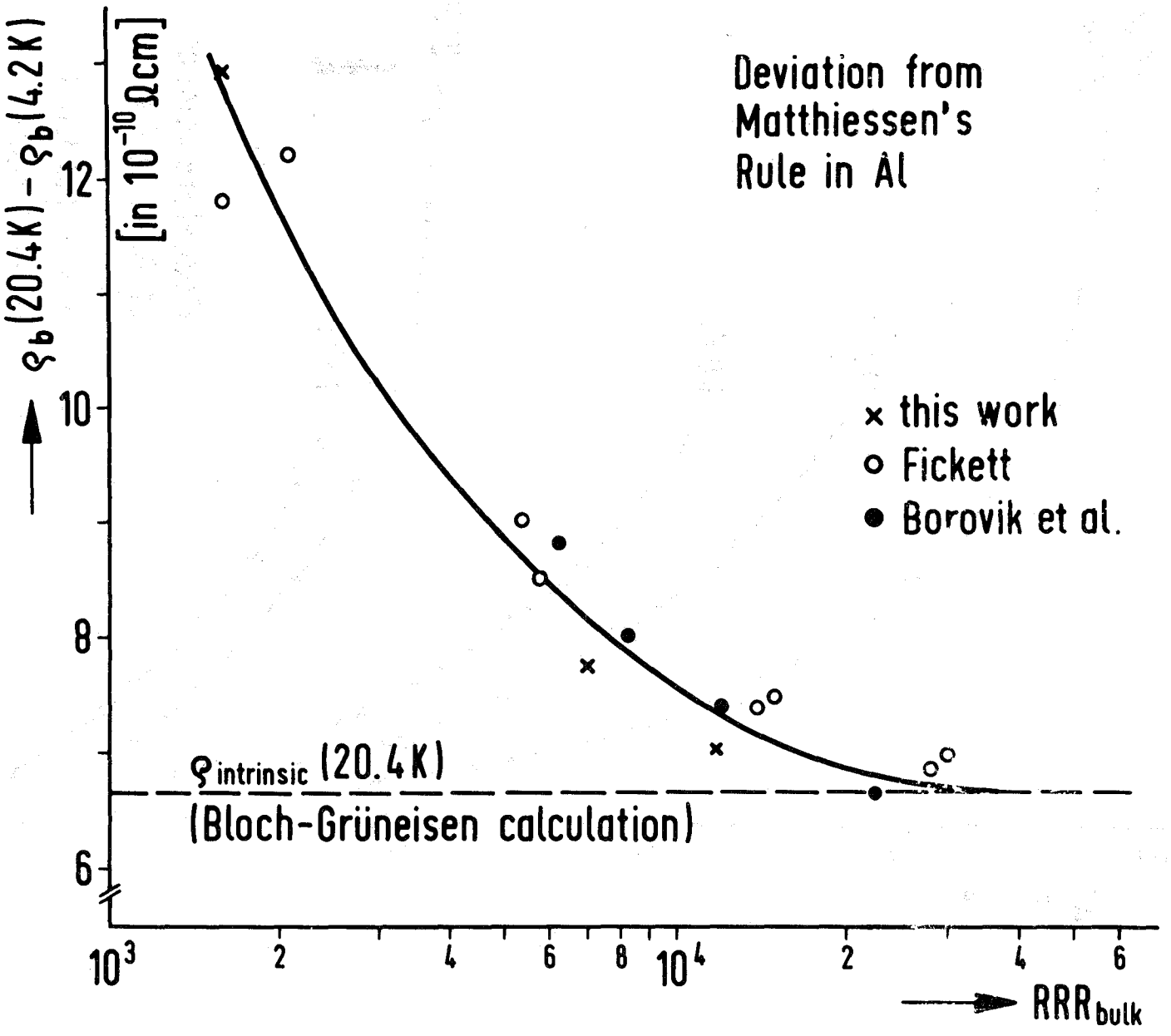
Deviation from
Matthiessen's
Rule in Al
× this work
o Fickett
● Borovik et al.
$\varrho_b(20.4K) - \varrho_b(4.2K)$ [in $10^{-10}\Omega cm$]
12
10
8
6
$\varrho_{intrinsic}$ (20.4 K)
(Bloch-Grüneisen calculation)
10^3
2
4
6
8
10^4
2
4
6
RRR_{bulk}

Fig. 9

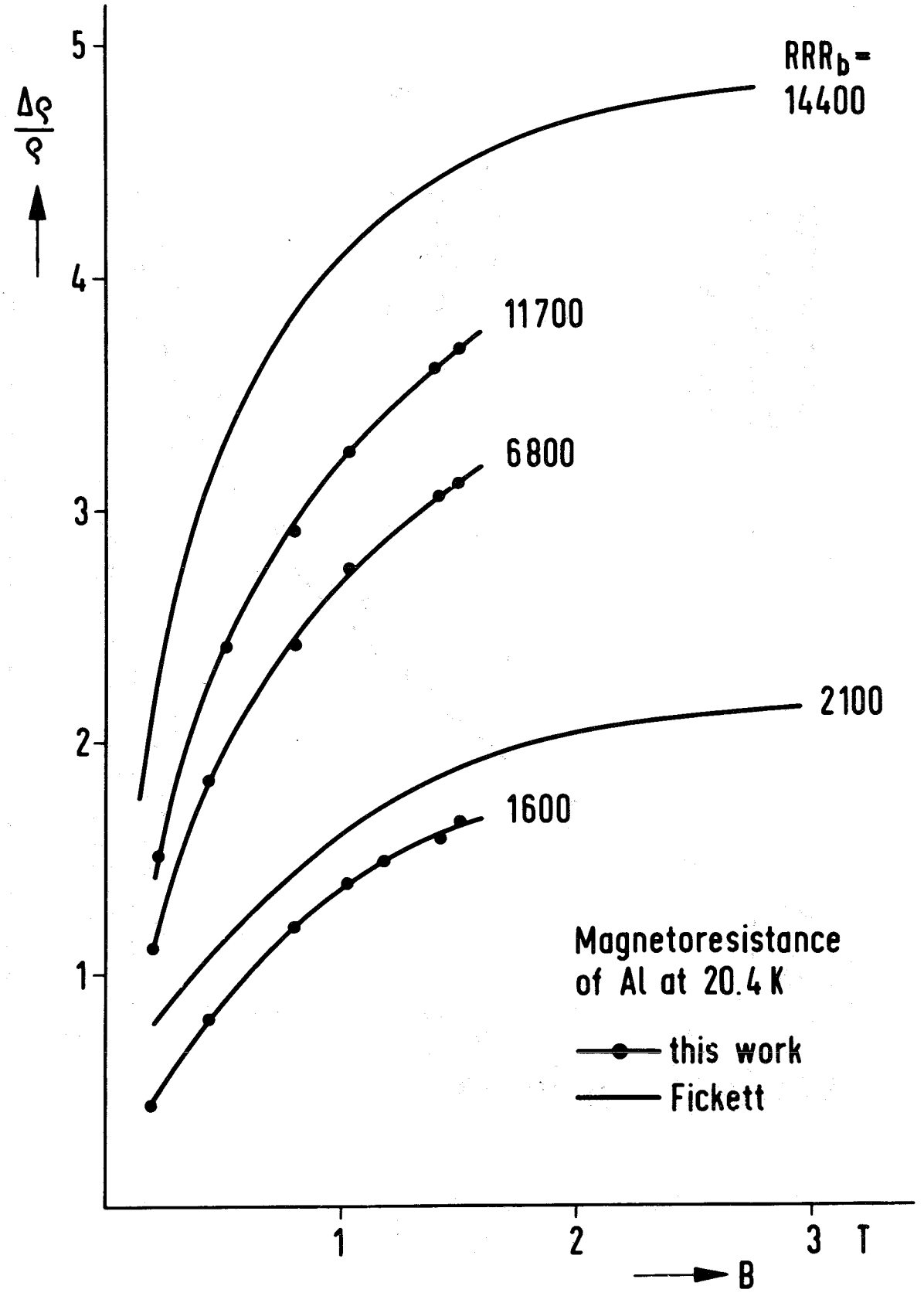
5
4
3
2
1
Δρ/ρ
RRR_b = 14400
11700
6800
2100
1600
Magnetoresistance of Al at 20.4 K
this work
Fickett
1
2
3 T
B

Fig. 10

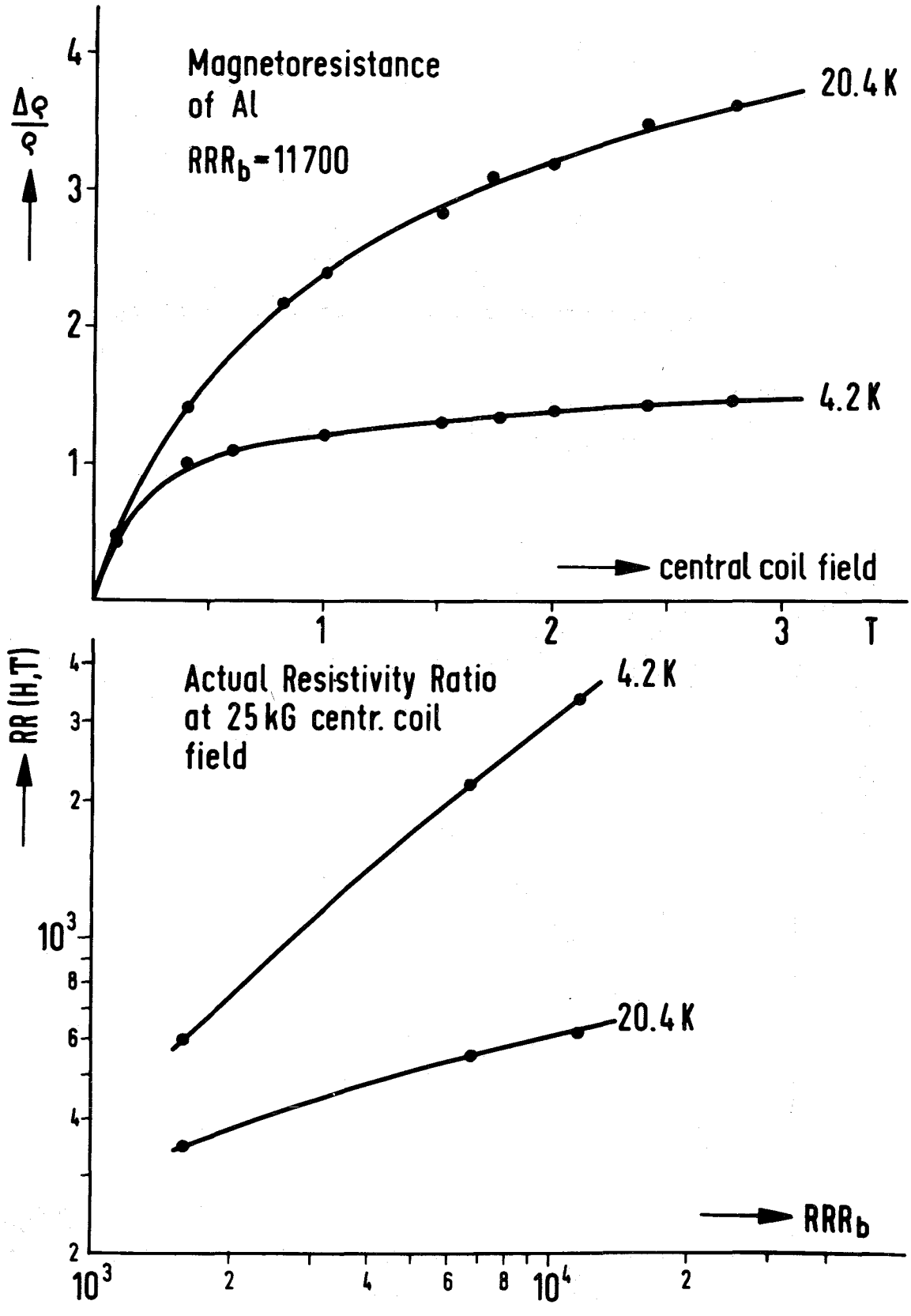
Magnetoresistance
of Al
RRR$_b$=11700
$\frac{\Delta\varrho}{\varrho}$
20.4 K
4.2 K
central coil field
T
Actual Resistivity Ratio
at 25 kG centr. coil
field
RR (H,T)
4.2 K
20.4 K
RRR$_b$

Fig. 11

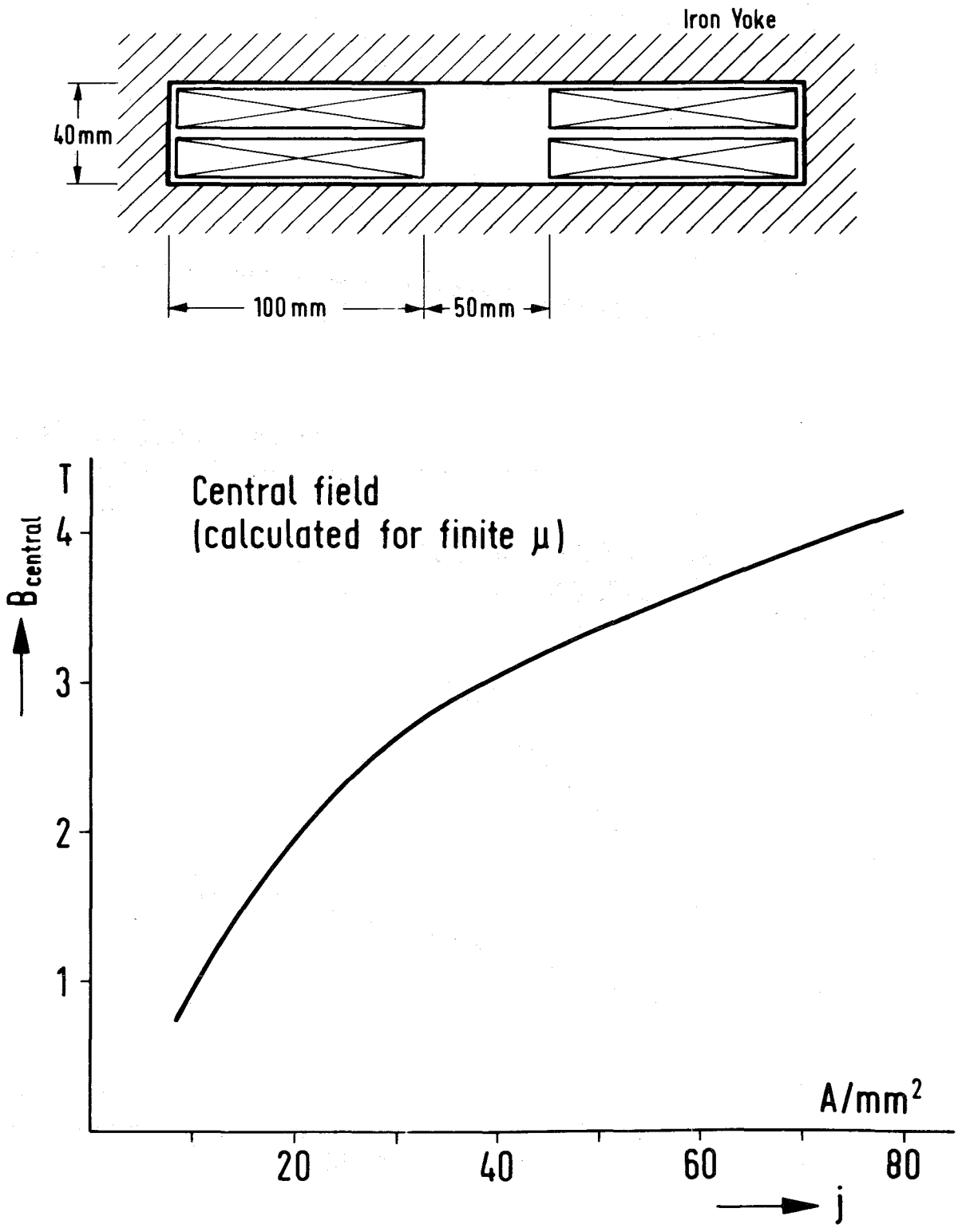
Al-TEST-MAGNET
Iron Yoke
40mm
100mm
50mm
Central field
(calculated for finite μ)
T
4
3
2
1
B central
A/mm²
20
40
60
80
j

Fig. 12